

Ferrimagnetic Mn_2SnO_4 nanowires

Chan Woong Na,^a Doo Suk Han,^a Jeunghye Park,^{*a} Younghun Jo^b and Myung-Hwa Jung^b

Received (in Cambridge, UK) 30th January 2006, Accepted 3rd April 2006

First published as an Advance Article on the web 25th April 2006

DOI: 10.1039/b601404f

Single-crystalline Mn_2SnO_4 nanowires were first synthesized by chemical vapor deposition; they consist of inverse spinel structure grown with the [111] direction; the nanowires have a ferrimagnetic phase below 46 K (T_C) with large hysteresis; this ferrimagnetic transition is probably due to the presence of Mn^{3+} ions at octahedral sites.

One-dimensional (1-D) nanostructures have attracted considerable attention due to the potential as building blocks for assembling active and integrated nanosystems.¹ Fabrication of nanodevices with novel function demands more diverse well-characterized 1-D nanostructures. Manganese stannate (Mn_2SnO_4) is a unique magnetic material, which is known to undergoes a ferrimagnetic transition at a Curie temperature (T_C) of 53–58 K, despite the expectation that it should be antiferromagnetic.^{2–4} Manganese stannate has an inverse spinel structure, symbolized as $\text{Mn}^{2+}[\text{Mn}^{2+}\text{Sn}^{4+}]_2\text{O}_4$, in which tetrahedral sites (A-sites) are occupied by Mn^{2+} ions, and octahedral sites (B-sites) by Mn^{2+} and Sn^{4+} ions. The origin of ferrimagnetic properties was suggested to be due to high-spin Mn^{3+} ions occupying B-sites.² Therefore this inverse spinel phase could be formulated as $\text{Mn}^{2+}[\text{Mn}^{2+}_{(1-b/2)}\text{Mn}^{3+}_b\text{Sn}^{4+}_{(1-b/2)}]_2\text{O}_4$.

The ferrimagnetism was also explained by a canting of the B-site moments.³ Further works suggested that Mn^{3+} ions are liable to induce, by a cooperative Jahn–Teller effect, a distortion of the cubic structure in the solid solution Mn_3O_4 – Mn_2SnO_4 .^{4,5} The Mn_2SnO_4 nanostructures are thus expected to be promising materials, not only for spintronic nanodevices, but also for an important question of how much difference of magnetic properties exists between bulk and nanosize materials. In the present work, we report for the first time the synthesis of single-crystalline Mn_2SnO_4 nanowires by chemical vapor deposition (CVD), and their unique ferrimagnetic properties, which are distinguished from those of the corresponding bulk phase.

MnCl_2 (99.99%, Aldrich) and Sn (99.8%, Aldrich) powders were placed in a source boat inside a quartz tube reactor. The silicon substrate was coated with an $\text{HAuCl}_4 \cdot 3\text{H}_2\text{O}$ (98+%, Sigma) ethanol solution, and then positioned on the source boat. High-density nanowires were grown on the substrates at 900–1000 °C, by 1 h reaction under oxygen flow. The products were analyzed by scanning electron microscopy (SEM, Hitachi S-4700), field-emission transmission electron microscopy (TEM, Jeol JEM 2100F), high-voltage TEM (HVEM, Jeol JEM ARM 1300S, 1.25 MV), energy dispersive X-ray fluorescence spectroscopy (EDX), and high-resolution X-ray diffraction (XRD) using the

8C2 beam line of the Pohang Light Source (PLS) with monochromatic radiation ($\lambda = 1.54520 \text{ \AA}$). X-Ray photoelectron spectroscopy (XPS, ESCALAB 250, VG Scientific) using a photon energy of 1486.6 eV ($\text{Al-K}\alpha$) was employed to investigate the electronic states. Magnetic properties were studied by a superconducting quantum interference device (SQUID, Quantum Design) magnetometer. Photoluminescence (PL) measurement was carried out using a He–Cd laser ($\lambda = 325 \text{ nm}$) as excitation source. Raman spectrum (Renishaw RM 1000) was measured using Ar ion laser ($\lambda = 514.5 \text{ nm}$).

Fig. 1(a) shows SEM images of high-density nanowires grown on a large area of Si substrate. A TEM image explicitly reveals the smooth surfaces and average diameter of 80 nm of the Mn_2SnO_4 nanowires (Fig. 1(b)). TEM images of selected nanowires and the corresponding ED pattern reveal a single-crystalline Mn_2SnO_4 cubic structure which grew in the [111] direction (Fig. 1(c) and inset). An atomic-resolved image shows a distance between neighboring (111) planes of ca. 5.1 Å (Fig. 1(d)), which is consistent with that of the bulk material ($a = 8.879 \text{ \AA}$; JCPDS No. 75-1516). All the nanowires that we observed have the [111] growth direction. EDX line-scanning reveals that the nanowires are composed of Mn, Sn and O, with an Mn:Sn ratio of ~2:1 (Fig. 1(e)). XRD patterns confirm that all products are pure Mn_2SnO_4 (Fig. 2). The peak position is consistent with that of JCPDS No. 75-1516. There are no peaks corresponding to

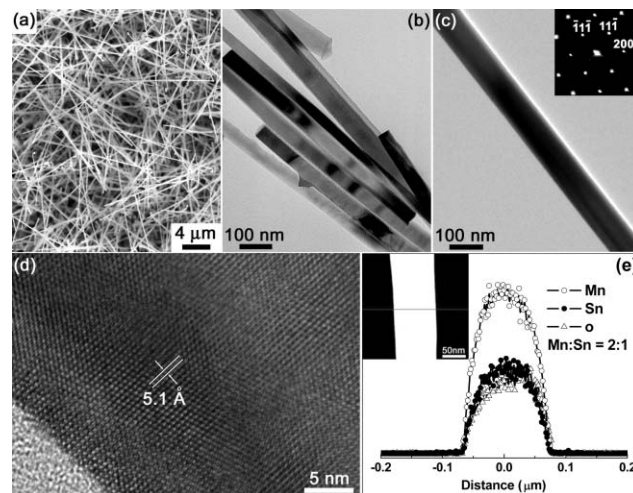


Fig. 1 (a) SEM micrograph of high-density Mn_2SnO_4 nanowires. (b) TEM image shows the uniform diameter of 80 nm. (c) TEM image and its corresponding ED pattern (inset) for a selected nanowire reveal single-crystalline Mn_2SnO_4 crystal and the [111] growth direction. (d) Atomic-resolved image shows that the distance between neighboring (111) planes is about 5.1 Å. (e) EDX line-scanning of Mn, O and Sn, for the cross section of the nanowire as shown in the inset.

^aDepartment of Chemistry, Korea University, Jochiwon, 339-700, Korea. E-mail: parkjh@korea.ac.kr; Fax: +82 2 3290 3992; Tel: +82 2 3290 3973

^bQuantum Material Research Team, Korea Basic Science Institute, Daejeon, 305-333, Korea

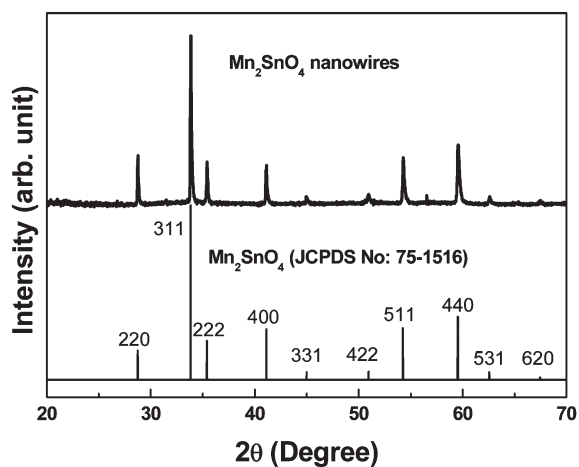


Fig. 2 XRD pattern of Mn_2SnO_4 nanowires along with the peaks of JCPDS No. 75-1516.

manganese oxide (e.g. Mn_3O_4 , MnO) or SnO_2 . These Mn_2SnO_4 nanowires would be grown by a vapor-liquid-solid mechanism, involving the Au nanoparticles deposited on the Si substrates.

Fig. 3(a) shows the full-range XPS spectrum comprising of Mn, O and Sn peaks. No contaminants other than C (from carbon tape) were detected. The ratio of Mn:Sn is approximately 2:1. Finely scanned Mn $2p_{1/2}$ and $2p_{3/2}$ peaks are displayed alongside those of MnO and Mn_3O_4 powders (Fig. 3(b)). The electronic state of Mn in Mn_2SnO_4 nanowires is close to that of Mn in tetragonal Mn_3O_4 , in which Mn^{2+} ions occupy A-sites and Mn^{3+} ions occupy B-sites. Therefore, our result suggests that Mn^{3+} ions may exist in

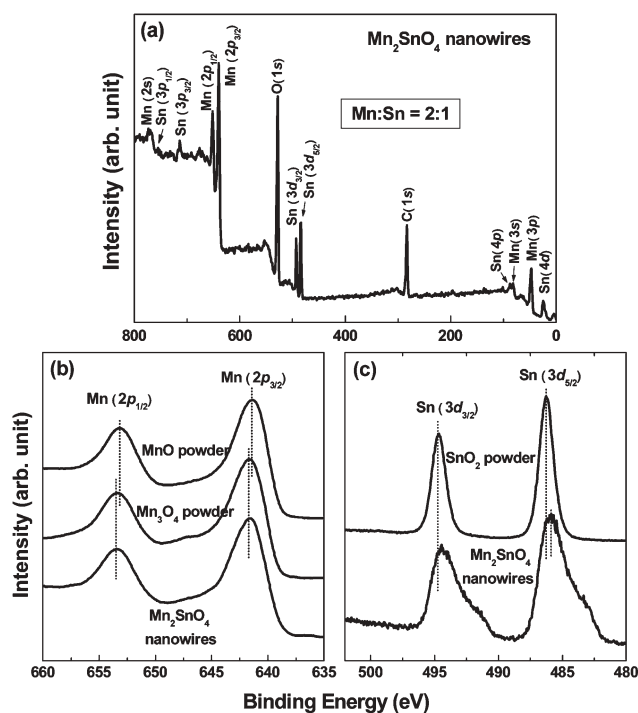


Fig. 3 (a) Full-range XPS spectrum showing Mn, O and Sn peaks. (b) Fine-scanned Mn $2p_{1/2}$ and $2p_{3/2}$ peaks of Mn_2SnO_4 nanowires are displayed alongside those of MnO and Mn_3O_4 powder. (c) Fine-scanned Sn $3d_{3/2}$ and $3d_{5/2}$ peaks are displayed alongside those of SnO_2 powder.

B-sites of Mn_2SnO_4 . Fine-scanned Sn $3d_{3/2}$ and $3d_{5/2}$ peaks are displayed alongside those of SnO_2 powder (Fig. 3(c)). The peak position shifts to lower energy vs. SnO_2 , and the width becomes broader with a shoulder at the lower energy side. The lower-energy shift, which corresponds to increased reduced levels, can be explained by the electronegativity (χ) difference between Sn^{4+} ($\chi_P = 1.96$) and Mn^{2+} ($\chi_P = 1.55$) ions. As the Sn^{4+} ions withdraw the electrons from the Mn^{2+} ions, the Mn^{2+} ions can be oxidized to Mn^{3+} ions. The broad electronic state of Sn suggests various reduced forms, probably due to inhomogeneous distribution among the sites.

Fig. 4(a) displays field-cooled (FC) and zero-field-cooled (ZFC) magnetization vs. temperature ($M-T$) curves in a field of 500 Oe. The high-temperature data exhibit paramagnetic behavior, whereas low-temperature data show a ferrimagnetic transition with $T_C = 46$ K. As has been reported, the origin of the ferrimagnetic nature could be associated with high-spin Mn^{3+} ions occupying B-sites.² The T_C of the nanowires is lower than that of the bulk (53–58 K).^{2–4} One possibility is that the present nanowires have a lower Mn^{2+} or Mn^{3+} content than the bulk. Earlier studies reported that the T_C of bulk Mn_2SnO_4 decreases as the number of Mn^{2+} ions decreases by the substitution of divalent ions,^{2,3} and the T_C of solid solutions Mn_3O_4 - Mn_2SnO_4 tends to increase as the content of Mn^{3+} ions increases.⁴ Unfortunately we cannot determine the content of Mn^{3+} ions from the magnetization, since the mass of nanowires is not exactly known and only estimated to be below 10^{-4} g. However, it is noteworthy that the T_C value is close to that of Mn_3O_4 nanowires, $T_C = 43$ K (bulk Mn_3O_4 has $T_C = 42$ K).⁶ Since the XPS data shows that the electronic structure of magnetic component Mn in Mn_2SnO_4 is close to that in Mn_3O_4 , the similar T_C would not be surprising. Therefore we presume that the nanowires would contain a high level of Mn^{3+} ions, which results from the oxidation of Mn^{2+} ions at the surface. Nevertheless the correlation between the Mn^{3+} content and T_C of the nanowires needs further investigation. Fig. 4(b) displays the magnetization vs. magnetic field ($M-H$) at different temperatures. Below 60 K the $M-H$ curves show hysteresis loops with large coercivity and remanence, which are indicative of ferrimagnetic components. The inset shows that the coercivity at 5 K is nearly 600 Oe.

Temperature-dependent (7–300 K) PL spectra of Mn_2SnO_4 nanowires were measured (Fig. 5). To the best of our knowledge, those have not been previously reported for Mn_2SnO_4 . At low

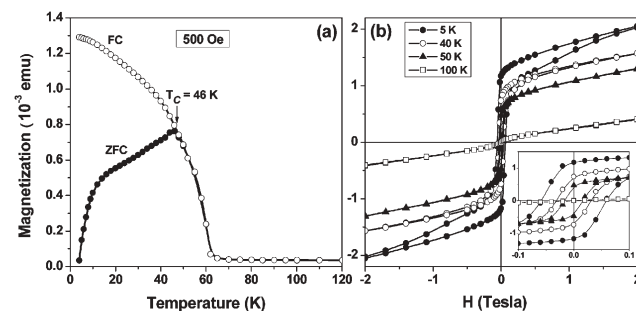


Fig. 4 (a) Temperature-dependent FC and ZFC magnetization of Mn_2SnO_4 nanowires measured in a magnetic field of 500 Oe. (b) $M-H$ curves measured at 5, 40, 50 and 100 K. Inset represents magnified scaled hysteresis loops near zero field.

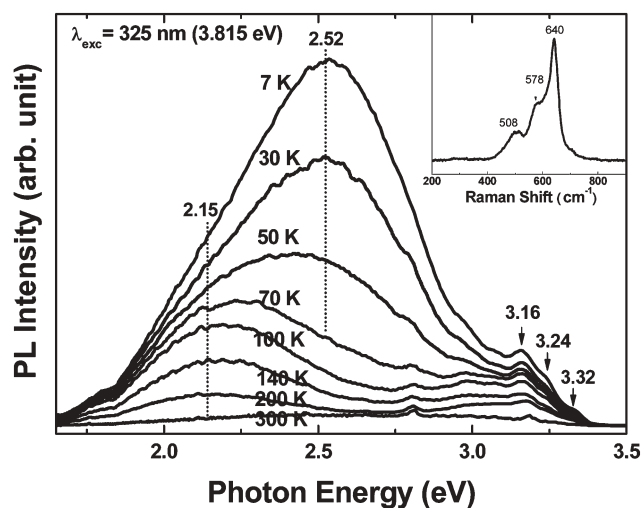


Fig. 5 Temperature-dependent PL spectrum of Mn_2SnO_4 nanowires. Inset represents their Raman spectrum.

temperatures a broad band appears at around 2.52 eV, which probably originates from the d–d (${}^4\text{T}_1 \rightarrow {}^6\text{A}_1$) transition of the tetrahedrally coordinated (A-site) Mn^{2+} ions. Mn-doped spinels, e.g., Zn_2SiO_4 , Mg_2SnO_4 , ZnGa_2O_4 , usually show green emission at 2.4–2.5 eV, coming from tetrahedrally coordinated Mn^{2+} ions.^{7–9} As the temperature increases, the peak intensity decreases significantly, and then another band centered at 2.15 eV becomes dominant. The Mn^{2+} ions present in B-sites would show a different form of crystal-field splitting, which may cause this red-shifted emission band. A series of peaks at 3.32, 3.24 and 3.16 eV, separated by 0.8 eV (644 cm^{-1}), was tentatively assigned to a zero phonon line and its phonon replicas of donor–acceptor pair emission. First-order Raman spectrum of Mn_2SnO_4 nanowires, reveals the corresponding vibrational mode 640 cm^{-1} (inset). Its peak position is close to that of the Mn–O lattice vibration frequency of Mn_3O_4 .¹⁰

In summary, we synthesized single-crystalline Mn_2SnO_4 nanowires by CVD. They consist of inverse spinel structure, grown with the [111] direction. The average diameter is 80 nm. XPS data reveal the existence of Mn^{3+} ions, which probably determine their ferrimagnetic behaviors. Magnetization measurements indicate that the Mn_2SnO_4 nanowires have a ferrimagnetic structure ($T_C = 46\text{ K}$), with significant hysteresis. The PL spectrum shows a broad band at around 2.52 eV, which originates from the d–d (${}^4\text{T}_1 \rightarrow {}^6\text{A}_1$) transition of the tetrahedrally coordinated Mn^{2+} ions. We suggest that Mn_2SnO_4 nanowires have a great deal of potential for applications in spintronic nanodevices.

This work was supported by KRF (Grant Nos. R14-2003-033-01003-0; R02-2004-000-10025-0; 2003-015-C00265), and KIST (Grant No. 2E18740-05-062). SEM, field-emission TEM, HVEM and SQUID measurements were performed at the Korea Basic Science Institute (Daejeon and Pusan). Experiments at PLS were supported in part by MOST and POSTECH.

Notes and references

- 1 J. Hu, T. W. Odom and C. M. Lieber, *Acc. Chem. Res.*, 1999, **32**, 435; M. S. Gudiksen, L. J. Lauhon, J. Wang, D. C. Smith and C. M. Lieber, *Nature (London)*, 2002, **415**, 617; X. Duan, Y. Huang, R. Agarwal and C. M. Lieber, *Nature (London)*, 2003, **421**, 241.
- 2 M. A. Gilleo and D. W. Mitchell, *J. Phys. Chem. Solids*, 1959, **10**, 182.
- 3 D. G. Wickham, N. Menyuk and K. Dwight, *J. Phys. Chem. Solids*, 1961, **20**, 316.
- 4 M. N. Poix, *Solid State Commun.*, 1974, **15**, 463.
- 5 M. Nagués and M. N. Poix, *J. Solid State Chem.*, 1974, **9**, 330.
- 6 C. W. Na, D. S. Han, D. S. Kim, J. Park, Y. T. Jeon, G. Lee and M. H. Jung, *Appl. Phys. Lett.*, 2005, **87**, 142504.
- 7 M. S. Kwon, C. J. Kim, H. L. Park, T. W. Kim and H. S. Lee, *J. Mater. Sci.*, 2005, **40**, 4089.
- 8 K. N. Kim, H. -K. Jung, H. D. Park and D. Kim, *J. Lumin.*, 2002, **99**, 169.
- 9 T. K. Tran, W. Park, J. W. Tomm, B. K. Wagner, S. M. Jacobsen, C. J. Summers, P. N. Yucom and S. K. McClelland, *J. Appl. Phys.*, 1995, **78**, 5691.
- 10 M.-C. Bernard, A. H. Goff, B. V. Thi and S. C. de Torresi, *J. Electrochem. Soc.*, 1993, **140**, 3065.